Progress In Electromagnetics Research, PIER 38, 253–267, 2002

FAST SOLUTION FOR LARGE SCALE ELECTROMAGNETIC SCATTERING PROBLEMS USING WAVELET TRANSFORM AND ITS PRECONDITION

X. C. Wei and E. P. Li

Computational Electromagnetics and Electronics Division
Institute of High Performance Computing
National University of Singapore
1 Science Park Road, Singapore Science Park II, Singapore 117528

C. H. Liang

Department of Electrical Engineering
Xidian University
Xi'an 710071, Shaanxi, China

Abstract—Nowadays, electrically large complex electromagnetic problems exist in modern defence and communication industry. Accurate and efficient calculation for such electromagnetic radiation and scattering is a high computational complex task and a challenge to conventional electromagnetic solvers such as Method of Moment (MOM) where high memory and long computational time are required owing to its large size compared to operating wavelength. This paper presents the fast solution method with wavelet transform in the computation of scattering from large scale complex objects. Because of the vanishing moments, the moment matrices arising in these problems are sparsified by wavelet, and consequently, the induced current and equivalent magnetic current can be obtained quickly. Moreover, a precondition method is postulated and implemented in the fast solution of the transformed moment matrix equation with iteration methods.

1. INTRODUCTION

The rapid growth in telecommunication and information systems over the past years, including advances in high frequency telecommunications, navigation, radar systems and computer networks, have created an enormous demand for modeling and simulation of more complicated structures and systems. Except for very simple systems, the electromagnetic analysis required for electrical performance assessment and for design of high performance telecommunication and information systems always results in large number of degrees of freedom, and therefore large number of unknowns in the electromagnetic model. Consequently, these large scale problems generally are beyond the range of applicability of many classical numerical algorithms due to computational complexity and huge memory requirements of these methods, as well as inadequate approximation models applied in these methods. In order to simulate complicated, large scale electromagnetic problems, the complexity of the applied techniques has to be reduced. In recent years a number of sophisticated fast numerical methods have been investigated at different stages of constructing an electromagnetic computational solver, including mathematical problem formulation, finite dimensional projection method and solving the discrete problem such as fast multipole method, fast Fourier Transfer method, model order reduction and etc.

For electrically large objects in radar cross section (RCS) computation, moment methods [1] with conventional expansion and testing functions results in large and dense matrix equations, direct solving of which is exhaustive. The fast solution method, wavelet transform, is applied to computing engineering to quickly sparsify dense matrices, and wavelet moment methods (WMM) is proposed to solve such electrically large problems [2–5].

This paper, in particular, presents the study on the fast wavelet transform method for computation of large scale electromagnetic scattering problem, and it is organised in the following. In Section 2, for the sake of clarify, a complete wavelet moment methods is introduced. In Section 3, the scattering from complicated objects is quickly solved using wavelet transform. In Section 4, a precondition method is proposed and implemented in reducing the condition numbers of transformed moment matrices.

2. WAVELET MOMENT METHODS

The electromagnetic field integral equation can be discretized by moment methods to the following matrix equation

$$\boldsymbol{Z} \cdot \boldsymbol{J} = \boldsymbol{E} \tag{1}$$

where $\boldsymbol{Z}$, $\boldsymbol{J}$ and $\boldsymbol{E}$ denote the $N \times N$ moment matrix, the induced current to be solved and the excitation vector, respectively. Now equation (1) is transformed by matrix $\boldsymbol{T}$ as following

$$\boldsymbol{Z}' = \boldsymbol{T} \cdot \boldsymbol{Z} \cdot \boldsymbol{T}^t, \quad \boldsymbol{J}' = \boldsymbol{T}^{-t} \cdot \boldsymbol{J}, \quad \boldsymbol{E}' = \boldsymbol{T} \cdot \boldsymbol{E} \tag{2}$$

where t denotes the matrix transpose, we can rewrite (1) as

$$\boldsymbol{Z}' \cdot \boldsymbol{J}' = \boldsymbol{E}' \tag{3}$$

Then (3) can be solved by iteration methods. This is the so-called wavelet moment methods and the matrix $\boldsymbol{T}$ is called the wavelet transform matrix. The cost of direct solvers such as gauss elimination method for (1) is $o(N^3)$. In order that the wavelet moment methods cost is less than it, $\boldsymbol{T}$ should satisfy the following criteria

1) The cost of transform $\boldsymbol{Z}' = \boldsymbol{T} \cdot \boldsymbol{Z} \cdot \boldsymbol{T}^t$ should be less than $o(N^3)$;
2) $\boldsymbol{Z}'$ should be spare. In what follows, the elements of $\boldsymbol{Z}'$ are thresholded with the level $\alpha \cdot \max\limits_{m,n} (|\boldsymbol{Z}(m,n)|)$, where $0 \le \alpha \le 1$. The sparsity rate is defined as the ratio of nonzero elements to total elements in the matrix;
3) $\boldsymbol{T}$ should be at least reversible in order that (3) is equivalent to (1), and the condition number of $\boldsymbol{Z}'$ should not be larger than that of $\boldsymbol{Z}$.

In the following, we will find out wavelet sequences, then the $\boldsymbol{T}$ meeting above criteria can be constructed by these sequences.

2.1. The Construction of Wavelet Sequences

Firstly, we define following 2×2 complex matrices $\boldsymbol{M}(z)$ and $\boldsymbol{N}(z)$

$$\begin{cases} \boldsymbol{M}(z) = \begin{bmatrix} P(z) & Q(z) \\ P(-z) & Q(-z) \end{bmatrix} \\[2ex] \boldsymbol{N}(z) = \begin{bmatrix} A(z) & A(-z) \\ B(z) & B(-z) \end{bmatrix}^* \end{cases} \tag{4}$$

where

$$\begin{cases} P(z) = \dfrac{1}{\sqrt{2}} \displaystyle\sum_{n=-\infty}^{\infty} p_n \cdot z^n \\[2ex] Q(z) = \dfrac{1}{\sqrt{2}} \displaystyle\sum_{n=-\infty}^{\infty} q_n \cdot z^n \\[2ex] A(z) = \dfrac{1}{\sqrt{2}} \displaystyle\sum_{n=-\infty}^{\infty} a_n \cdot z^n \\[2ex] B(z) = \dfrac{1}{\sqrt{2}} \displaystyle\sum_{n=-\infty}^{\infty} b_n \cdot z^n \end{cases} \tag{5}$$

in which, $z = e^{-j\omega}$, $\omega \in R$, R represents the real assemble, j denotes the square root of -1, $*$ denotes the conjugate. Sequences $\{p_n\}$, $\{q_n\}$, $\{a_n\}$ and $\{b_n\} \in R$, they are the wavelet sequences to be solved and their length are finite.

Then we define $N \times N$ real matrices $\boldsymbol{W}_N$ and $\boldsymbol{V}_N$

$$\boldsymbol{W}_N = \begin{array}{r} \\ 1 \\ \\ \\ \\ \\ \\ \frac{N}{2} \\ \frac{N}{2}+1 \\ \\ \\ \\ \\ \\ N \end{array} \begin{array}{l} 1 \qquad\qquad\qquad\qquad\qquad\qquad\qquad\qquad\qquad N \\ \left[\begin{array}{l} a_0\ a_1\ a_2\ \cdots\ a_m\ 0 \cdots\cdots\cdots 0 \\ 0\ \ 0\ \ a_0\ a_1\ a_2\ \cdots\ a_m\ 0 \cdots\cdots 0 \\ \cdots\cdots\cdots\cdots\cdots\cdots\cdots\cdots \\ 0 \cdots\cdots 0\ a_0\ a_1\ a_2\ \cdots\ a_m \\ a_{m-1}\ a_m\ 0 \cdots 0\ a_0\ a_1\ a_2\ \cdots\ a_{m-2} \\ \cdots\cdots\cdots\cdots\cdots\cdots\cdots\cdots \\ a_2\ a_3\ a_4\ \cdots a_m\ 0 \cdots\cdots 0\ a_0\ a_1 \\ b_0\ b_1\ b_2\ \cdots\ b_n\ 0 \cdots\cdots\cdots 0 \\ 0\ \ 0\ \ b_0\ b_1\ b_2\ \cdots\ b_n\ 0 \cdots\cdots 0 \\ \cdots\cdots\cdots\cdots\cdots\cdots\cdots\cdots \\ 0 \cdots\cdots 0\ b_0\ b_1\ b_2\ \cdots\ b_n \\ b_{n-1}\ b_n\ 0 \cdots 0\ b_0\ b_1\ b_2\ \cdots\ b_{n-2} \\ \cdots\cdots\cdots\cdots\cdots\cdots\cdots\cdots \\ b_2\ b_3\ b_4\ \cdots b_n\ 0 \cdots\cdots 0\ b_0\ b_1 \end{array} \right] \end{array} \tag{6}$$

$$
\boldsymbol{V}_N = \begin{array}{r@{\;}c}
 & \begin{array}{lcr} 1 & \qquad\qquad\qquad\qquad\qquad\qquad & N \end{array} \\
\begin{array}{r} 1 \\ \\ \\ \\ \\ \\ \frac{N}{2} \\ \frac{N}{2}+1 \\ \\ \\ \\ \\ \\ N \end{array} &
\left[\begin{array}{l}
p_0\ p_1\ p_2\ \cdots\ p_k\ 0 \cdots\cdots 0 \\
0\ \ 0\ \ p_0\ p_1\ p_2\ \cdots\ p_k\ 0 \cdots\cdots 0 \\
\cdots\cdots\cdots\cdots\cdots\cdots\cdots\cdots\cdots \\
0 \cdots\cdots 0\ p_0\ p_1\ p_2\ \cdots\ p_k \\
p_{k-1}\ p_k\ 0 \cdots\cdots 0\ p_0\ p_1\ p_2\ \cdots\ p_{k-2} \\
\cdots\cdots\cdots\cdots\cdots\cdots\cdots\cdots\cdots \\
p_2\ p_3\ p_4\ \cdots p_k\ 0 \cdots\cdots 0\ p_0\ p_1 \\
q_0\ q_1\ q_2\ \cdots\ q_l\ 0 \cdots\cdots 0 \\
0\ \ 0\ \ q_0\ q_1\ q_2\ \cdots\ q_l\ 0 \cdots\cdots 0 \\
\cdots\cdots\cdots\cdots\cdots\cdots\cdots\cdots\cdots \\
0 \cdots\cdots 0\ q_0\ q_1\ q_2\ \cdots\ q_l \\
q_{l-1}\ q_l\ 0 \cdots\cdots 0\ q_0\ q_1\ q_2\ \cdots\ q_{l-2} \\
\cdots\cdots\cdots\cdots\cdots\cdots\cdots\cdots\cdots \\
q_2\ q_3\ q_4\ \cdots q_l\ 0 \cdots\cdots 0\ q_0\ q_1
\end{array}\right]
\end{array} \tag{7}
$$

where, the row vectors of $\boldsymbol{W}_N$ and $\boldsymbol{V}_N$ are the cycle translates of sequences $\{a_n\}$, $\{b_n\}$, $\{p_n\}$ and $\{q_n\}$ with 2 as the step in the interval $[1, N]$, the subscript N denotes the matrix rank.

So that, the conclusion is made that [3]

$$\boldsymbol{N}(z) \cdot \boldsymbol{M}(z) = \boldsymbol{I} \tag{8}$$

is equivalent to

$$\boldsymbol{W}_N \cdot \boldsymbol{V}_N^t = \boldsymbol{I}_N \tag{9}$$

Where $\boldsymbol{I}_N$ denotes the $N \times N$ real identity matrix.

We will use $\boldsymbol{W}_N$ and $\boldsymbol{V}_N$ to construct $\boldsymbol{T}$. So $\{p_n\}$, $\{q_n\}$, $\{a_n\}$ and $\{b_n\}$ must satisfy Equation (8) in order that $\boldsymbol{W}_N$, $\boldsymbol{V}_N$, and $\boldsymbol{T}$ are at least reversible. At the same time, in order that $\boldsymbol{Z}'$ is sparse, $\{b_n\}$ and $\{q_n\}$ should have some vanishing moments. We say that the sequence $\{x_n\}$ has M-order vanishing moments if and only if

$$\sum_{n=-\infty}^{\infty} x_n n^i = 0, \qquad i = 0, 1, \ldots, M-1 \tag{10}$$

and $\sum_{n=-\infty}^{\infty} x_n n^M \neq 0$.

When $\{b_n\}$ and $\{q_n\}$ have some vanishing moments, the multiplication between these sequences and the matrix in which the row and column vectors vary slowly yields a sparse vector. This is the reason that the wavelet transform matrix $\boldsymbol{T}$ can make matrix $\boldsymbol{Z}'$ sparse. On the other hand, these sequences length increase when their vanishing moments increase. There is a relationship between the vanishing moments of wavelet sequences and their polynomials $P(z)$, $A(z)$, $B(z)$ and $Q(z)$ as following [3].

$P(z)$ (or $A(z)$) should include the factor $(z+1)^M$ in order that $\{b_n\}$ (or $\{q_n\}$) has M-order vanishing moments.

There are two kind of wavelet sequences often used in computation: for orthonormal wavelet sequences such as Daubechies sequence and Haar sequence [6], they satisfy the Equations (8), the additional conditions are that $P(z) = A(z)$, and $\{q_n\}$, $\{b_n\}$ both have M-order vanishing moments; for double-orthonormal wavelet sequences [7], they satisfy the Equation (8), the additional conditions are that $\{p_n\}$ and $\{a_n\}$ are symmetric sequences respectively, and $\{q_n\}$ and $\{b_n\}$ have M_1-order and M_2-order vanishing moments respectively. With these additional conditions we can find out the solutions of (8).

2.2. The Construction of Wavelet Transform Matrix $\boldsymbol{T}$

Now we can define following $N \times N$ real matrices

$$\boldsymbol{T}_1 = \boldsymbol{W}_N,\ \boldsymbol{T}_2 = \begin{bmatrix} \boldsymbol{W}_{\frac{N}{2}} & 0 \\ 0 & \boldsymbol{I}_{\frac{N}{2}} \end{bmatrix},\ \boldsymbol{T}_3 = \begin{bmatrix} \boldsymbol{W}_{\frac{N}{4}} & 0 \\ 0 & \boldsymbol{I}_{\frac{3N}{4}} \end{bmatrix}, \ldots,$$
$$\boldsymbol{T}_m = \begin{bmatrix} \boldsymbol{W}_{\frac{N}{2^{m-1}}} & 0 \\ 0 & \boldsymbol{I}_{N-\frac{N}{2^{m-1}}} \end{bmatrix} \tag{11}$$

Let $\boldsymbol{T} = \boldsymbol{T}_m \cdot \boldsymbol{T}_{m-1} \ldots \boldsymbol{T}_1$. If we use $\boldsymbol{V}_N$ to take the place of $\boldsymbol{W}_N$ in (11), the daul matrix of $\boldsymbol{T}$ is obtained as $\tilde{\boldsymbol{T}}$.

Provided the length of $\{a_n\}$ and $\{p_n\}$ both are l, from (11) we can see that in wavelet moment methods the total multiplication number of those transforms (2) is $4l(1-\frac{1}{2^m})(N^2+N)$, which costs only $o(N^2)$. Because of the vanishing moments of wavelet sequences, the matrix $\boldsymbol{Z}'$ is sparse. From the discussion above we can see that for orthonormal wavelet matrix, $\boldsymbol{T}^{-1} = \boldsymbol{T}^t$, while for double-orthonormal wavelet matrix, $\boldsymbol{T}^{-1} = \tilde{\boldsymbol{T}}^t$, so Equation (3) is equivalent to (1). At this moment, the wavelet matrix $\boldsymbol{T}$ obtained satisfies all the three criteria above. It should be noted that, in [8], it is shown that the condition number of $\boldsymbol{Z}'$ may become worse than that of $\boldsymbol{Z}$ after double-orthonormal wavelet transform. So we prefer to use orthonormal sequences rather than using double-orthonormal sequences in this paper.

3. SOLUTION OF SCATTERING PROBLEMS

From above section, we can see that the wavelet transform can be taken as a matrix transform. So it can be widely used in scattering problems. In the following, it is used to solve linear equations in the scattering from a cube, then, it is used to find out the inside admittance matrix in the scattering from a cavity. Here, all scatters analyzed are assumed as perfect electric objects. The dimension of scatters are uniformed by λ (λ is the wavelength of the incident plane wave).

3.1. The Solution of Induced Current for a Cube

For the cube, electromagnetic field integral equation is

$$\vec{\boldsymbol{E}}^i(\vec{\boldsymbol{r}})_t = \left[j\omega\vec{\boldsymbol{A}}(\vec{\boldsymbol{J}}_s) + \nabla\Phi(\vec{\boldsymbol{J}}_s)\right]_t \qquad \vec{\boldsymbol{r}} \in s \tag{12}$$

where, t denotes the tangential component to S, S is the surface of the cube, and $\vec{\boldsymbol{A}}$, Φ are the vector potential and scalar potential respectively [9], $\vec{\boldsymbol{J}}_s$ is the induced current to be solved, $\vec{\boldsymbol{E}}^i(\vec{\boldsymbol{r}})$ is the incident electric field.

Rao's patches with the area of $0.005\lambda^2$ are used as expansion and test functions to discretify (12) and generate moment matrices [9]. There are four cubes with different size to be considered as shown in Figure 1.

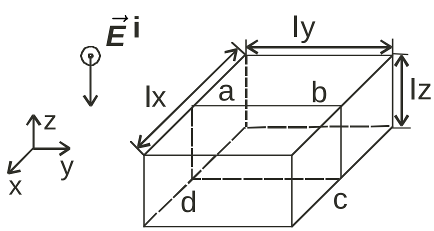

Figure 1. The cube and the TM incident wave.

Cube 1: $l_x = l_y = 0.4\lambda,\ l_z = 0.2\lambda$;
Cube 2: $l_x = 0.6\lambda,\ l_y = l_z = 0.4\lambda$;
Cube 3: $l_x = l_y = 0.8\lambda,\ l_z = 0.4\lambda$;
Cube 4: $l_x = 1.2\lambda,\ l_y = l_z = 0.8\lambda$.

It is well known that the integral kernel of (12) is the free-space Green function and its differential, which are strongly singular. So with the Rao's patches, the magnitude of row and column vectors in moment matrices $\boldsymbol{Z}$ have sharp pulses as shown in Figure 2. Because

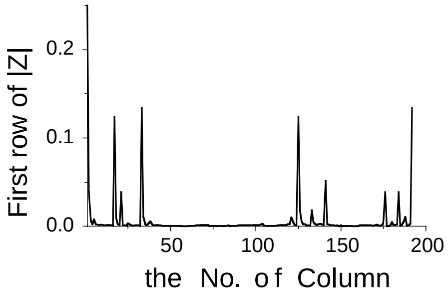

Figure 2. The first row of $|\boldsymbol{Z}|$ for cube 1.

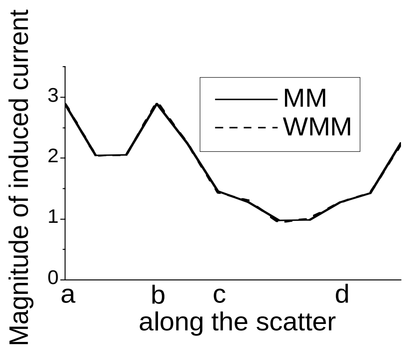

Figure 3. Distribution of the induced current of wavelet transform method and conventional moment methods for cube 1.

most Daubechies sequences are longer than Haar sequence, Haar sequence can generate more sparse $\boldsymbol{Z}'$ in 3-D problems than Daubechies sequences do, although it has lower order vanishing moments, which can be verified in the following examples.

Now (12) can be discretized to Equation (1). After the orthonormal wavelet transform, we can get Equation (3). In radar cross section computation, since there are many incident vectors for one moment matrix, it is convenient to find out the $\boldsymbol{Z}^{-1}$ rather than to solve the Equation (1) each time when the incident vector is changed. For the same reason, we will find out $\boldsymbol{Z}'^{-1}$ in (3). Because $\boldsymbol{Z}'^{-1} = (\boldsymbol{T}\cdot \boldsymbol{Z}\cdot \boldsymbol{T}^t)^{-1} = \boldsymbol{T}\cdot \boldsymbol{Z}^{-1}\cdot \boldsymbol{T}^t$, so $\boldsymbol{Z}'^{-1}$ is sparse also. The induced current can be obtained by $\boldsymbol{J} = \boldsymbol{T}^t \cdot \boldsymbol{Z}'^{-1} \cdot \boldsymbol{E}'$.

Figure 3 shows the induced current for cube 1, which is perpendicular to the line abcd shown in Figure 1, by using wavelet transform method (Haar sequence is used, WMM) and conventional moment methods(MM). We can see that the results are well correlated.

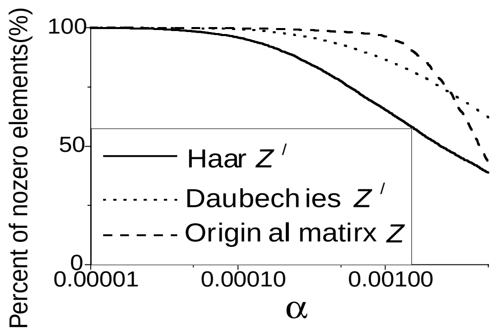

Figure 4. Percent of nonzero elements in $\boldsymbol{Z}$ and $\boldsymbol{Z}'$.

Table 1. The CPU time and the error of wavelet transform method and conventional moment methods for cubes.

Cubes		1	2	3	4
Generate $\boldsymbol{Z}$ (Sec.)		0.44	1.65	5.11	18.78
MM(sec.) Find out $\boldsymbol{Z}^{-1}$ and $\boldsymbol{J}$		4.23	39.22	405.46	3276.20
WMM (Sec.)	Transform	0.05	0.16	0.71	2.96
	Find out $\boldsymbol{Z}'^{-1}$ and $\boldsymbol{J}$	2.53	28.23	293.85	2437.71
Relative error (%)		2.91	2.83	2.53	2.64

Figure 4 shows the variation of percent of nonzero elements in $\boldsymbol{Z}$, $\boldsymbol{Z}'$ after 8-order Daubechies sequence transform and $\boldsymbol{Z}'$ after Haar sequence transform with the threshold value α. Here the scatter is the cube 1. We can see that $\boldsymbol{Z}'$ associated with Haar sequence is more sparse than that associated with Daubechies sequence and the original matrix $\boldsymbol{Z}$. For other cubes the same results can be obtained.

Table 1 shows the CPU time required to obtain induced current of cubes by using wavelet transform methods(Haar sequence is used) and conventional moment methods. Where, the relative error refers to $||\boldsymbol{J}_{MM} - \boldsymbol{J}_{\boldsymbol{WMM}}||_2/||\boldsymbol{J}_{MM}||_2$, $\boldsymbol{J}_{\boldsymbol{MM}}$ and $\boldsymbol{J}_{\boldsymbol{WMM}}$ denote the current obtained by wavelet transform method and conventional moment methods respectively. From table 1 we can see that the total CPU time of wavelet transform method including transform and finding out $\boldsymbol{Z}'^{-1}$ and $\boldsymbol{J}$ is less than that of conventional moment methods, and the relative error between them are small. The outstanding advantage of the Haar sequence is its less transform time which can be ignored compared with the conventional moment methods time.

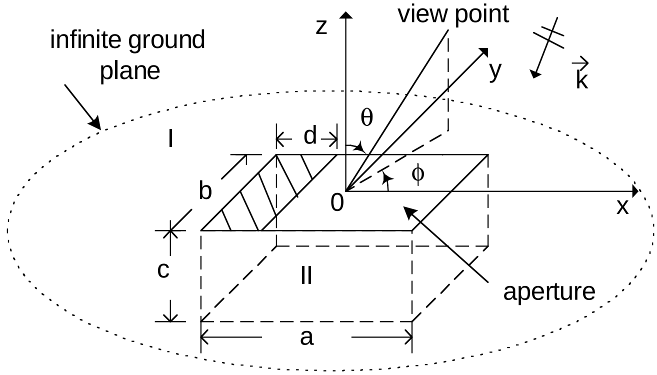

Figure 5. Partially open cavities and the incident wave.

3.2. The Solution of Scattering from Partially Open Cavities

The scattering from partially open cavities recessed in an infinite ground plane is analyzed with Haar sequence. The scatter and incident wave are shown in Figure 5. This problem can be solved by using equivalent magnetic current method [10]. As shown in Figure 5, the geometry can be divided into an inside and an outside region with the aperture as the common boundary. Then the equivalent magnetic currents are placed on two sides of this aperture. By matching the magnetic field over the aperture, an integral equation can be obtained. The integral equation can further be discretized to the following matrix equation

$$(\boldsymbol{Y}_{out} + \boldsymbol{Y}_{in}) \cdot \boldsymbol{V} = \boldsymbol{I} \tag{13}$$

where, $\boldsymbol{I}$ denotes the incident magnetic field over the aperture, $\boldsymbol{V}$ denotes the unknown equivalent magnetic current, $\boldsymbol{Y}_{out}$ and $\boldsymbol{Y}_{in}$ are the admittance matrices of the outside and inside region respectively. These two matrices can be formulated independently. $\boldsymbol{Y}_{out}$ can be easily obtained by free-space Green function and $\boldsymbol{Y}_{in}$ can be obtained by boundary-integral equation. In order to find out $\boldsymbol{Y}_{in}$, we partition the cavity internal walls and the aperture into square patches and get the $\boldsymbol{Y}_{in}$ matrix of the form

$$\boldsymbol{Y}_{in} = -\left(\boldsymbol{A}_{aa} - \boldsymbol{A}_{ac} \cdot \boldsymbol{A}_{cc}^{-1} \cdot \boldsymbol{A}_{ca}\right)^{-1} \cdot \left(\boldsymbol{B}_{aa} - \boldsymbol{A}_{ac} \cdot \boldsymbol{A}_{cc}^{-1} \cdot \boldsymbol{B}_{ca}\right) \tag{14}$$

where, the subscript c and a denote the cavity internal walls and the aperture respectively, matrices $\boldsymbol{A}_{mn}$ and $\boldsymbol{B}_{mn}$ are obtained by the discretization of the boundary-integral equation, $m,\ n = a$ or c. For simplicity, here we do not give their complicated expressions which can

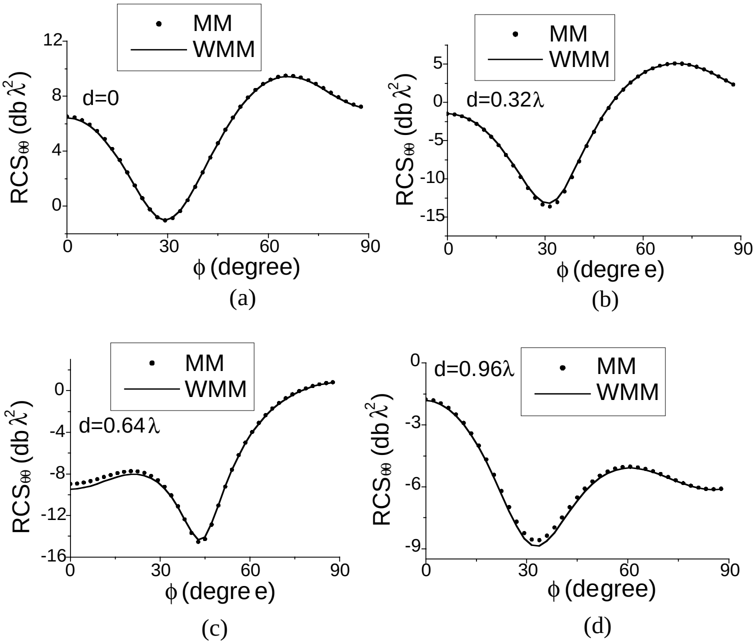

Figure 6. Radar cross section for wavelet transform method and conventional moment methods.

be found in [10]. $\boldsymbol{A}_{cc}^{-1}$ is needed in order to get $\boldsymbol{Y}_{in}$ from (14). The size of $\boldsymbol{A}_{cc}$ is $2(N-K)\times 2(N-K)$, where K is the number of patches on the aperture, and N is the total number of patches on the aperture and cavity internal walls. For these cavities in this problem, N is very large and K is very small, so $\boldsymbol{A}_{cc}$ is dense and large. It is exhaustive to find out $\boldsymbol{A}_{cc}^{-1}$ directly. Now we use Haar wavelet matrix $\boldsymbol{T}$ to make $\boldsymbol{A}_{cc}$ sparse, so $\boldsymbol{Y}_{in}$ can be quickly got. With the help of $\boldsymbol{T}$, (14) can be rewritten as

$$\begin{aligned}\boldsymbol{Y}_{in} &= -\left(\boldsymbol{A}_{aa} - \left(\boldsymbol{A}_{ac}\boldsymbol{T}^t\right)\cdot\left(\boldsymbol{T}\boldsymbol{A}_{cc}\boldsymbol{T}^t\right)^{-1}\cdot\left(\boldsymbol{T}\boldsymbol{A}_{ca}\right)\right)^{-1}\\ &\quad\cdot\left(\boldsymbol{B}_{aa} - \left(\boldsymbol{A}_{ac}\boldsymbol{T}^t\right)\cdot\left(\boldsymbol{T}\boldsymbol{A}_{cc}\boldsymbol{T}^t\right)^{-1}\cdot\left(\boldsymbol{T}\boldsymbol{B}_{ca}\right)\right)\\ &= -\left(\boldsymbol{A}_{aa}-\boldsymbol{A}'_{ac}\cdot{\boldsymbol{A}'_{cc}}^{-1}\cdot\boldsymbol{A}'_{ca}\right)^{-1}\cdot\left(\boldsymbol{B}_{aa}-\boldsymbol{A}'_{ac}\cdot{\boldsymbol{A}'_{cc}}^{-1}\cdot\boldsymbol{B}'_{ca}\right)\end{aligned} \tag{15}$$

Because $\boldsymbol{A}'_{cc}$ is sparse, the CPU time for ${\boldsymbol{A}'_{cc}}^{-1}$ is less than that for $\boldsymbol{A}_{cc}^{-1}$.

There are four cavities to be examined with $d = 0,\ 0.32\lambda,\ 0.64\lambda$

and 0.96λ respectively. Let $b = c = 0.8\lambda$, $a = 1.28\lambda$ and the width of square patches are 0.08λ for all cavities. Figure 6 shows the radar cross section in $\theta\theta$ pattern obtained by using two methods: one get $\boldsymbol{Y}_{in}$ from Equation (15) (WMM) and the other get $\boldsymbol{Y}_{in}$ from Equation (14) (MM). Here θ and ϕ are the azimuthal and polar angles of the view point. Let $\theta = 40°$ for all of these four cavities. It can be seen from Figure 6 that the agreement between two methods are good. The wavelet transform methods error only results from the numerical approximation during $\boldsymbol{Z}'$ is thresholded, it dose not result from the physically approximation such as high frequency methods, so the error arising in wavelet transform can be small when the threshold value α is chosen to be small.

Table 2. The sparsity rate of $\boldsymbol{A}'_{cc}$ and the CPU time of wavelet transform method and conventional moment methods for cavities.

d (λ)	Find out $\boldsymbol{A}_{cc}^{-1}$ (Sec.)	WMM		
		Transform (Sec.)	Find out $\boldsymbol{A}'^{-1}_{cc}$ (Sec.)	Sparsity rate of $\boldsymbol{A}'_{cc}$ (%)
0	1849.29	5.44	975.06	22.64
0.32	2406.95	6.98	1669.02	31.34
0.64	2641.86	5.16	1504.85	33.85
0.96	3905.64	5.38	2498.24	38.98

Table 2 shows the sparsity rate of $\boldsymbol{A}'_{cc}$ and the CPU time of wavelet transform method and conventional moment methods. Again, we see that the total CPU time of wavelet transform method is less than that of conventional moment methods, and the transform time is less because Haar sequence is used.

4. A PRECONDITION METHOD FOR WAVELET MOMENT METHODS

As discussed in Section 2, the condition number of the moment matrix does not change after the orthonormal wavelet transform. In order that Equation (3) can be solved more quickly by such iteration methods as the conjugate gradient method, $\boldsymbol{Z}'$ with smaller condition number is expected. As we can see from all literatures about wavelet moment methods that the large elements of $\boldsymbol{Z}'$, which strongly affect the eigenvalue contribution of $\boldsymbol{Z}'$, are located in the left-up and diagonal of $\boldsymbol{Z}'$ [2–5, 8]. According to this characteristic of $\boldsymbol{Z}'$, Equation (3) can

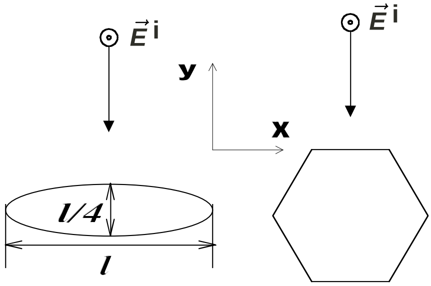

Figure 7. Cylinders and the TM incident wave.

be transformed by using the precondition matrix $\boldsymbol{P}$ as following

$$\boldsymbol{Z}'_p \cdot \boldsymbol{J}'_p = \boldsymbol{E}'_p \tag{16}$$

where, $\boldsymbol{Z}'_p = \boldsymbol{P}^{-1} \cdot \boldsymbol{Z}' \cdot \boldsymbol{P}^{-1}$, $\boldsymbol{J}'_p = \boldsymbol{P} \cdot \boldsymbol{J}'$, $\boldsymbol{E}'_p = \boldsymbol{P}^{-1} \cdot \boldsymbol{E}'$. $\boldsymbol{P}$ is a diagonal matrix, of which the elements are the square root of the elements at the diagonal of $\boldsymbol{Z}'$ (get the one which has less phase). $\boldsymbol{P}$ can make $\boldsymbol{Z}'_p$ more well-conditioned than $\boldsymbol{Z}'$ and the transform time for (16) is less because $\boldsymbol{P}$ and $\boldsymbol{Z}'$ are very sparse, so (16) can be solved more quickly by the conjugate gradient method than (3). The performance of the precondition method is tested through the solution of the induced current of ellipse cylinders and hexagon cylinders under TM incidence. The scatters and incident wave are shown in Figure 7. The size of moment matrices are 512×512 for ellipse cylinders and 768×768 for hexagon cylinders. Moment matrices are generated with pulse base and point matching. By changing the width of pulse functions, we can obtain moment matrices for cylinders with different size. Here the Daubechies sequence with the order 8 is used to generate Equation (3).

Table 3 and Table 4 show the improvement on the condition number of $\boldsymbol{Z}'$ and the conjugate gradient method convergence rate for ellipse cylinders and hexagon cylinders respectively due to the precondition. From tables we can see that after the precondition, the condition number of $\boldsymbol{Z}'$ becomes smaller and the iteration number of the conjugate gradient method becomes less. So the CPU time of precondition method can be reduced compared with the non-precondition method. This improvement is more obvious when the width of pulse functions is small. Because of the ill-posedness of electrical field integral equation, when the width of pulse functions becomes small, $\boldsymbol{Z}$ becomes more ill-conditioned, which greatly slows down the conjugate gradient method convergence [11]. In this case, the precondition method is very useful in reducing the condition number

Table 3. The improvement on the condition number of $\boldsymbol{Z}'$ and the conjugate gradient method convergence rate for ellipse cylinders.

$l\,(\lambda)$		3.84	6.4	8.96	11.52	14.08
Non-precondition	Condition number of $\boldsymbol{Z}'$	238.08	187.67	163.60	160.90	127.87
	Iteration number for solving (3):n_1	147	162	172	206	194
	Relative error(%)	2.73	3.00	3.31	3.47	4.76
Precondition	Condition number of $\boldsymbol{Z}'_p$	46.61	43.73	66.86	209.50	64.76
	Iteration number for solving (16):n_2	42	57	72	108	106
	Relative error(%)	2.73	3.00	3.31	3.47	4.76
n_1/n_2		3.5	2.84	2.39	1.91	1.83

Table 4. The improvement on the condition number of $\boldsymbol{Z}'$ and the conjugate gradient method convergence rate for hexagon cylinders.

Width of pulse functions(λ)		0.02	0.04	0.06	0.08	0.1
Non-precondition	Condition number of $\boldsymbol{Z}'$	89.01	46.87	211.09	59.16	235.67
	Iteration number for solving (3):n_1	130	116	177	125	256
	Relative error(%)	7.36	5.40	6.73	6.00	8.06
Precondition	Condition number of $\boldsymbol{Z}'_p$	14.97	12.47	242.41	57.35	210.36
	Iteration number for solving (16):n_2	46	36	99	106	181
	Relative error(%)	7.36	5.40	6.73	6.00	8.06
n_1/n_2		2.83	3.22	1.79	1.18	1.41

of $\boldsymbol{Z}'$ or improving the eigenvalue distribution of $\boldsymbol{Z}'$. The relative error in Tables 3 and 4 refer to the induced current error between the one obtained by solving (1) directly and the one obtained by solving (3) or (16) using conjugate gradient method. Because the acceptable relative error for stopping iteration is the same for these two methods, their relative error is the same.

5. CONCLUSION

The fast wavelet transform method has been successfully implemented in the scattering computation for large scale and complicated objects. It has been shown through numerous examinations that the computating time is dramatically reduced with the accelerating of the fast wavelet transform. Also, a precondition method is provided to reduce the condition number of transformed moment matrices.

REFERENCES

1. Harrington, R. F., *Field Computation by Moment Methods,* Macmillan Company, New York, 1968.
2. Steinberg, B. Z. and Y. Leviatan, "On the use of wavelet expansions in the method of moments," *IEEE Trans. Antennas Propagat.,* Vol. 41, 610–619, 1993.
3. Wei, X. C., "Application of wavelet analysis to computational electromagnetics," Ph.D. thesis, Xi'an, P.R.C., 2001.
4. Wagner, R. L. and W. C. Chew, "A study of wavelets for the solution of electromagnetic integral equations," *IEEE Trans. Antennas Propagat.,* Vol. 43, 802–810, 1995.
5. Golik, W. L., "Wavelet packets for fast solution of electromagnetic integral equations," *IEEE Trans. Antennas Propagat.,* Vol. 46, 618–624, 1998.
6. Chui, C. K., *An Introduction to Wavelets,* San Diego, Academic Press, USA, 1992.
7. Daubechies, I., *Ten Lectures on Wavelets,* SIAM Publ., Philadelphia, 1992.
8. Wei, X. C. and C. H. Liang, "A comparison between the applications of orthonormal wavelet and dualorthonormal wavelet for the wavelet moment methods," *Journal of Microwave (Chinese),* Vol. 16, 384–388, 2000.
9. Rao, S. M., D. R. Wilton, and A. W. Glisson, "Electromagnetic scattering by surface of arbitrary shape," *IEEE Trans. Antennas Propagat.,* Vol. 30, 409–418, 1982.
10. Wang, T. M. and H. Ling, "Electromagnetic scattering from three-dimension cavities via a connection scheme," *IEEE Trans. Antennas Propagat.,* Vol. 39, 1505–1513, 1991.
11. Peterson, A. F., C. F. Smith, and R. Mittra, "Eigenvalues of the moment-method matrix and their effect on the convergence of the conjugate gradient algorithm," *IEEE Trans. Antennas Propagat.,* Vol. 36, 1177–1179, 1988.